

# Estimating coarse root biomass with ground penetrating radar in a tree-based intercropping system

Kira A. Borden · Marney E. Isaac ·  
Naresh V. Thevathasan · Andrew M. Gordon ·  
Sean C. Thomas

Received: 26 September 2013 / Accepted: 3 June 2014 / Published online: 14 June 2014  
© Springer Science+Business Media Dordrecht 2014

**Abstract** Conventional measurements of tree root biomass in tree-based intercropping (TBI) systems can be inadequate in capturing the heterogeneity of rooting patterns or can be highly destructive and non-repeatable. In this study, we estimated coarse root biomass using ground penetrating radar (GPR) of 25-year-old trees inclusive of five species (*Populus deltoides* × *nigra* clone DN-177, *Juglans nigra* L., *Quercus rubra* L., *Picea abies* L. Karst, and *Thuja occidentalis* L.) at a TBI site in Southern Ontario, Canada. Subsurface images generated by GPR were collected in grids (4.5 × 4.5 m) centred on tree stems. The predictive relationship developed between GPR signal response and root biomass was corrected for species effects prior to tree-scale estimates of below-ground biomass. Accuracy of the tree-scale estimates

was assessed by comparing coarse root biomass measured from complete excavations of the corresponding tree. The mean coarse root biomass estimated from GPR analysis was  $54.1 \pm 8.7$  kg tree<sup>-1</sup> (mean ± S.E.;  $n = 12$ ), within 1 % of the mean coarse root biomass measured from excavation. Overall there was a root mean square error of 14.4 kg between measured and estimated biomass with no detectable bias despite variable conditions within the in-field and multi-species study. Root system C storage by species, calculated with species-specific root carbon concentrations, is estimated at  $5.4 \pm 0.7$ – $34.8 \pm 6.9$  kg C tree<sup>-1</sup> at this site. GPR is an effective tool for non-destructively predicting coarse root biomass in multi-species environments such as temperate TBI systems.

K. A. Borden · S. C. Thomas  
Faculty of Forestry, University of Toronto, Toronto, ON,  
Canada

K. A. Borden · M. E. Isaac  
Department of Geography, University of Toronto,  
Toronto, ON, Canada

M. E. Isaac (✉)  
Department of Physical and Environmental Sciences,  
University of Toronto Scarborough, Toronto,  
ON M1C 1A4, Canada  
e-mail: marney.isaac@utoronto.ca

N. V. Thevathasan · A. M. Gordon  
School of Environmental Sciences, University of Guelph,  
Guelph, ON, Canada

**Keywords** Temperate agroforestry · Belowground biomass · Root detection · Geo-imaging · Tree root system · Volatile carbon · Carbon storage

## Introduction

With more than 20 % of total tree biomass allocated belowground, tree roots comprise a substantial but understudied component of biomass in many ecosystems (Cairns et al. 1997; Mokany et al. 2006; Brunner and Godbold 2007). Ecological benefits derived from the presence of tree roots, particularly in modified

agricultural systems, include soil amelioration via root exudation, turnover, and sloughing, improved water infiltration and aeration from root channels, and prevention of erosion (Schroth 1999; Jose et al. 2004; Thevathasan and Gordon 2004; Jose 2009; Nair et al. 2009). Furthermore, the incorporation of trees into agricultural landscapes can increase the C storage potential, considerably within belowground biomass, and is touted as a viable and potentially significant land-use approach to sequester atmospheric CO<sub>2</sub> (Dixon et al. 1994; Isaac et al. 2005; Peichl et al. 2006; Bambrick et al. 2010; Kuyah et al. 2012). While potential aboveground C sequestration in temperate agroforestry systems is estimated at  $1.9 \times 10^9$  Mg C year<sup>-1</sup> (Oelbermann et al. 2004), data are limited on the belowground contribution. Improved approaches to estimate and predict the belowground biomass are required to fully capture the role of roots in C budgets for temperate TBI.

Biomass inventories within agroforestry systems are primarily focused on measuring the aboveground component with a limited number of studies also calculating root mass (e.g. Oelbermann et al. 2005; Peichl et al. 2006; Kirby and Potvin 2007; Moser et al. 2010; Kessler et al. 2012). Conventional sampling techniques of tree root systems include minirhizotrons, profile walls, and soil cores (Vogt et al. 1998; Polomski and Kuhn 2002). However, due to the spatial heterogeneity and the inherent fractal nature of root systems, these techniques generally have low accuracy particularly for coarse roots (diameter > 2 mm) (Schroth and Kolbe 1994; Taylor et al. 2013). Conversely, partial or complete root system excavations are time consuming, destructive, and non-repeatable. This has led to the wide utilization of root:shoot ratios (e.g. Jackson et al. 1996; Cairns et al. 1997; Mokany et al. 2006) or allometric equations (e.g. Kurz et al. 1996; Jenkins et al. 2003) generated from biomass studies in forest ecosystems. However, such broad generalizations of tree biomass allocation may produce inaccuracies when applied to agroforestry, or TBI sites specifically, due to variation in tree root growth in cultivated scenarios (Nair 2011; Kuyah et al. 2012). Thus, there is a need for new methodologies to study and measure root biomass in TBI systems.

Ground penetrating radar (GPR) emits electromagnetic (EM) signals into the ground and records the reflected EM waves' amplitude, polarity, and travel time. Signal reflections occur where there is a contrast

in dielectric permittivity in the subsurface (Davis and Annan 1989). Importantly, water has a high dielectric constant (Davis and Annan 1989) and when coarse roots contain greater water content than the surrounding soil matrix, the necessary contrast of dielectric properties for radar signal reflections is met (Hruska et al. 1999; Hirano et al. 2009; Guo et al. 2013b, c). As a GPR unit operates along a transect, the reflected signals can be compiled to create an interpreted image, or radargram, of the subsurface with signal reflections at a root (perpendicularly orientated to the GPR transect) depicted as a hyperbolic reflection pattern (Barton and Montagu 2004). Depth of GPR signal penetration is limited by the antenna frequency of the GPR unit and the electrical conductivity of the subsurface (Davis and Annan 1989). The water and clay content of the soil will also influence the rate of radar signal attenuation due to their dielectric properties (Butnor et al. 2001). Ideal conditions for GPR study of coarse roots are well-drained soils with low clay content and with coarse roots of sufficient water content (Guo et al. 2013a).

A key benefit of GPR estimation of root biomass is that it provides researchers the opportunity for repeated measurements of coarse roots and the capacity to examine the uniqueness of tree root system responses along gradients of biotic and abiotic constraints (Isaac and Anglarea 2013). Previous studies on the use of GPR for biomass estimation have involved controlled experiments (Barton and Montagu 2004; Dannoura et al. 2008; Hirano et al. 2009; Cui et al. 2013; Guo et al. 2013c; Tanikawa et al. 2013) and in situ testing within tree monocultures or two-species mixtures (Butnor et al. 2003; Stover et al. 2007; Samuelson et al. 2008, 2010; Hirano et al. 2012; Raz-Yaseef et al. 2013; Day et al. 2013). Generally, physical samples of root biomass equating to corresponding areas of GPR radargrams have been compared to develop predictive relationships between a GPR signal response index and root biomass (Butnor et al. 2003; Stover et al. 2007; Guo et al. 2013a). A growing body of research has used this approach to explore root responses to variation in atmospheric CO<sub>2</sub> (Stover et al. 2007; Day et al. 2013), forest stand management techniques (Butnor et al. 2003; Samuelson et al. 2008, 2010), and precipitation patterns (Raz-Yaseef et al. 2013). However, the utility of GPR biomass estimation has yet to be tested in a multi-species scenario or in an agroforestry system

specifically. Also, prior GPR studies have not derived estimates of root biomass for individual trees, or specifically applied GPR to estimates of root carbon. Therefore, the objectives of the present study were to test the utility of GPR for coarse root biomass estimation across a variety of tree species under field conditions, and to estimate the C content of individual trees in a temperate TBI system.

## Materials and methods

### Study site

Ground penetrating radar data and root samples were collected below 13 individual trees at the University of Guelph Agroforestry Research Station, Guelph, Ontario, Canada (44°32′28″N, 80°12′32″W; elevation 325 m). The 30-ha site was established in 1987 as an experimental TBI system. A variety of tree species are planted in tree rows that are spaced 12.5 or 15 m apart, in between which a conventional crop rotation is practiced under no-till cultivation and annual intercropping of *Zea mays* L. (maize), *Glycine max* (L.) Merr. (soybean), *Triticum aestivum* L. (winter wheat), or *Hordeum vulgare* L. (barley) (Thevathasan and Gordon 2004).

The soil is classified as Grey-Brown Luvisol with a sandy loam texture (65 % sand, 25 % silt, and 10 % clay) (Oelbermann and Voroney 2007). The A<sub>p</sub> horizon continues to a depth of 28–53 cm (Price and Gordon 1999) and a moraine till is located approximately 1 m below the soil surface.

The 13 studied trees were of five species that are commonly selected for agroforestry systems in the region: *Populus deltoides* × *nigra* clone DN177 (hybrid poplar; DBH = 33.5 ± 0.6 cm; *n* = 2), *Juglans nigra* L. (black walnut; DBH = 24.8 ± 1.0 cm; *n* = 3), *Quercus rubra* L. (red oak; DBH = 21.3 ± 0.5 cm; *n* = 3), *Picea abies* L. Karst. (Norway spruce; DBH = 21.5 ± 3.5 cm; *n* = 2), all with aboveground heights >7 m, and the multi-stem *Thuja occidentalis* L. (eastern white cedar; DBH = 9.1 ± 2.3 cm; *n* = 3)<sup>1</sup>, with aboveground height >4 m. The trees were planted with 6 m in-row tree stem spacing, except *T. occidentalis* with 1 m spacing. Each of the

five tree species studied were replicated with 2 or 3 randomly selected individuals. All trees in the study were approximately 25 years old and were located in flat areas of the site.

### Radar survey

The area around the base of each target tree was cleared of leaf litter and other organic material. A 4.5 × 4.5 m grid frame was installed surrounding the base of each target tree so the tree stem was situated in the approximate centre (Fig. 1a). The grid frame was constructed of plastic pipe, which served to anchor guide-rope at 10 cm increments in both the x and y directions (Fig. 1b). To ensure straight and square transects, the GPR unit was pulled by an attached handle so that the antennae remained alongside the grid guide-rope. Data collection below 13 trees occurred between April and June, 2012. Transect increments of 10 cm were selected for GPR data collection to reduce dependency on interpolation. Each set of tree GPR data were collected on the same day and under consistent conditions with the GPR programmed to EM signal emission intervals of 0.1 ns stacked with 16 traces every 0.5 cm along each transect.

To measure the average EM signal velocity in the subsurface, metal rods were inserted horizontally at depths of 40 cm into soil profiles adjacent to target trees. The signal travel time and distance of the GPR antenna to the rods were measured and thus average velocity of the radar signal was calculated. Velocities were measured the day of data collection for each tree and ranged between 0.08 and 0.10 m ns<sup>-1</sup>.

Tree root detection typically occurs with a GPR antenna emitting a centre frequency of 500 MHz (e.g. Barton and Montagu 2004) up to 2,000 MHz (e.g. Cui et al. 2013). For this study, we used a 1,000 MHz GPR unit (NogginPlus; Sensors and Software Inc., Mississauga, ON, Canada) for all data collection. Previous studies using this frequency have reported detection coarse roots of diameter 0.5 cm and greater (Guo et al. 2013a).

Water content of coarse roots and soil within study plots was determined by weighing samples before and after drying at 65 °C for 7 days. Coarse root gravimetric and volumetric water contents (assuming cylindrical root shapes) were 175 ± 7 and 76 ± 1 % (mean ± S.E.; *n* = 65), respectively, inclusive of all

<sup>1</sup> DBH of *T. occidentalis* is the mean ± S.E. of the largest stem from the primary trees located in study plots.

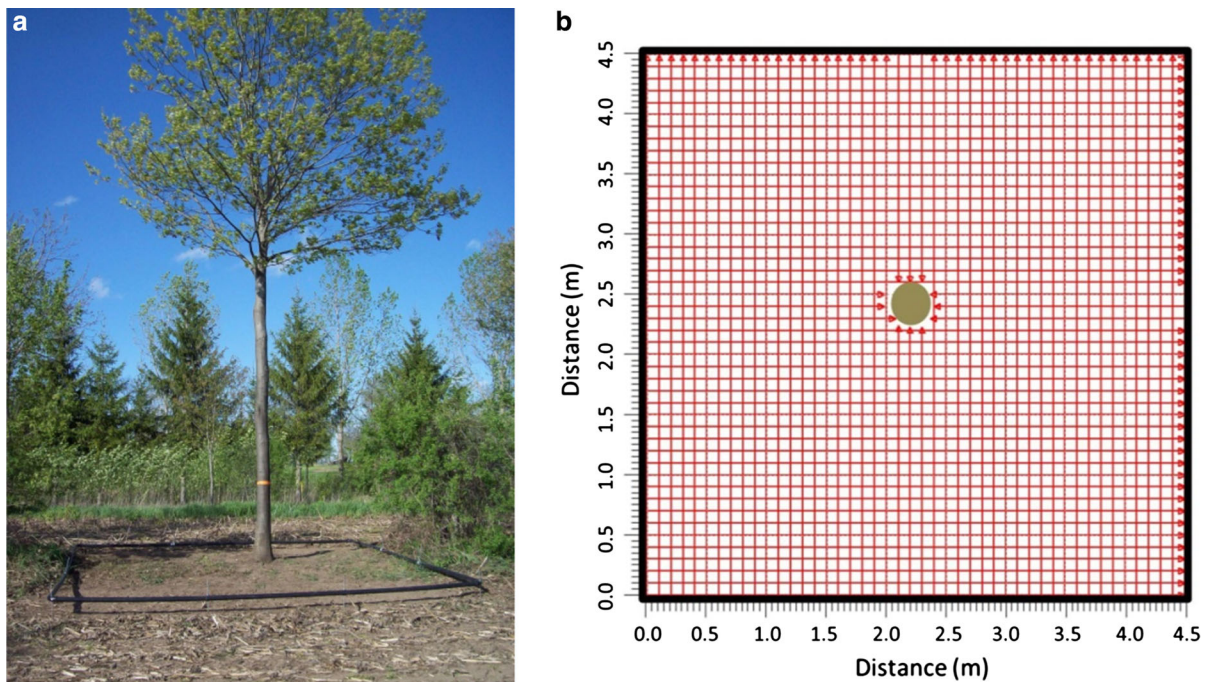


**Fig. 1** **a** Image of grid set-up for GPR survey of *Quercus rubra* in tree-based intercropping system at the University of Guelph Agroforestry Research Station, Guelph, Ontario, Canada. **b** Plan-view schematic of GPR data collection grid design.

study trees ( $n = 10$  or  $15$  per species). The soil gravimetric and volumetric water contents (using known soil sampler volume of 100 mL) to a depth of 60 cm over the entire study period were  $10 \pm 1$  and  $12 \pm 5 \%$  (mean  $\pm$  S.E.;  $n = 20$ ), respectively. Thus, the necessary soil to root water content gradient was satisfied for GPR detection and interpretation (Hirano et al. 2009; Guo et al. 2013c) with coarse roots containing greater than six times more water than the soil on a volume basis.

#### Radargram processing

Prior to image analysis of the GPR data, non-root anomalies (e.g. plane reflectors and signal “noise”) were reduced with a sequence of image processing steps (DC shift, dewow, and background removal) (Fig. 2b, c). Subsequently, dipping features, such as hyperbolic reflections of roots, were repositioned to their foci with a migration algorithm (2d FK migration with *Stolt* equation using known signal velocity and the angle of incidence) (Fig. 2d). Finally, an envelope algorithm known as the *Hilbert* transformation (operating on

The base of tree stem is represented by the *circle* located in the centre of the grid. *Red lines* indicate GPR data collection transects in x and y directions with 10 cm spacing. (Color figure online)

amplitudes of the reflected EM waves are used to interpret the data into one phase) was applied so that reflectors are more discernible (Fig. 2e). In order to enhance subsurface root reflections representatively with depth, a spreading and exponential compensation gain (SEC2) was applied to all processed GPR radargrams based on the rate of energy decay, similar to methodology in Cui et al. (2013) and Guo et al. (2013c). A colour palette of bipolar grey was selected for visualization whereby low to high amplitude response was displayed as grey to white. All GPR data processing steps were completed in EKKO\_View Deluxe (Sensors and Software Inc.).

Ground penetrating radar radargrams were imported into ImageJ (US National Institutes of Health, Bethesda, MD, USA) as 8-bit bmp files with pixel intensities ranging between 0 and 255. Radargrams were standardized to ensure consistent measures of distance within an image using a ratio of 400 pixels: 1 m. The final data processing step measured the number of pixels within an established threshold range (175–255) and subsequently converted to a cross-sectional area ( $\text{cm}^2$ ) (Fig. 2f), defined as the GPR index.

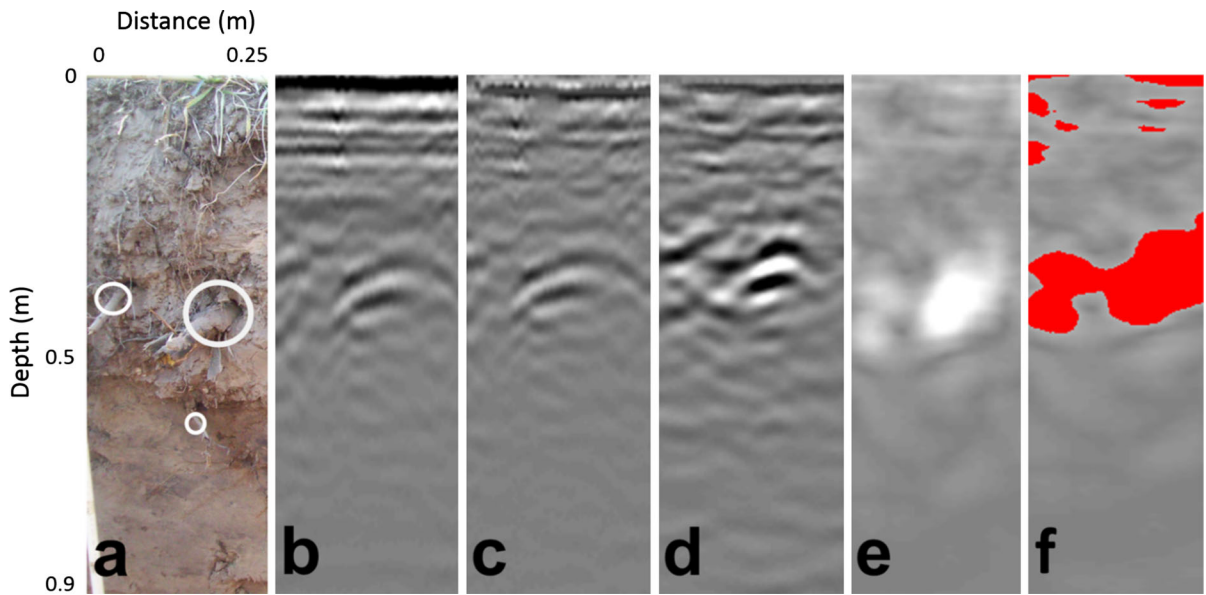


**Fig. 2** GPR data processing sequence with soil profile (0.25 × 1.0 m) and exposed roots (*circles*) of *Juglans nigra* (a) and the equivalent GPR geo-image (b) with applied background removal (c) surface reflections or banding is reduced. Hyperbola migration focuses root reflections to foci

(d). The final data processing step is the *Hilbert* transformation whereby magnitude of reflection is brought into one phase (e). The extracted GPR index (area within an intensity range (175–255 cm<sup>2</sup>) is measured (f) to develop a GPR index–biomass relationship

**Table 1** Relational equations between specific root biomass (W) representing dry weight (g) of 10 cm long root segments with root diameter (D) (cm) (*n* = 20 per species)

Tree species	Biomass relationship to diameter <sup>a</sup>	<i>r</i>
<i>Populus</i> sp.	$W = 2.9138 \times D^{1.8183}$	0.9959
<i>J. nigra</i>	$W = 3.5694 \times D^{1.933}$	0.9936
<i>Q. rubra</i>	$W = 4.9623 \times D^{1.8976}$	0.9980
<i>P. abies</i>	$W = 3.7016 \times D^{1.8715}$	0.9993
<i>T. occidentalis</i>	$W = 3.0168 \times D^{1.8269}$	0.9901

<sup>a</sup> It was assumed that root diameter was constant for 10 cm to be comparable to GPR transect spacing of 10 cm

**GPR index–biomass relationship**

Following GPR data collection, soil profiles (0.25 m across and 1 m deep) were exposed at distances ranging from 0.5 to 2.0 m from the tree stem (*n* = 64) (Fig. 2a). These soil profiles were orientated along GPR data transects and included all study trees (*n* = 4 or 6 profiles per tree). To calculate total coarse root dry weight biomass in each excavated soil profile, the diameters of all coarse roots crossing through the exposed profiles were measured and applied to species-specific relationships of root dry weight

biomass to root diameter as described in Hirano et al. (2012) and Guo et al. (2013b) (Table 1). Relationships were developed from root samples (*n* = 20 per species) of various diameters collected at all study trees and assumed a root length of 10 cm, which is equivalent to the GPR transect spacing.

To determine the GPR index, three pixel intensity thresholds (165–255, 175–255, and 200–255) were selected based on visually delineating root features and minimizing the inclusion of non-root anomalies. The area derived from each threshold level were compared for their correlations to coarse root biomass. The pixel intensity threshold of 175–255 (Fig. 2f) was ultimately selected to generate the area index of GPR signal response as it produced the optimal correlation with measured biomass.

**Coarse root biomass estimates**

The radargram processing sequence was applied to all GPR data within each tree grid. The resulting GPR index determined for each transect was used to calculate the predicted root biomass using the GPR index–biomass relationship. All transect biomass estimates were summed for total tree coarse root

biomass ( $B_{\text{GPR}}$ ;  $\text{kg tree}^{-1}$ ). Since tree roots are best detected when crossing between  $45^\circ$  and  $135^\circ$  to the plane of the radargram (Butnor et al. 2001; Tanikawa et al. 2013), the biomass estimates from grid transects in both  $x$  and  $y$  directions were included to maximize root detection by capturing roots irrespective of direction of growth.

Ground penetrating radar results were compared to an estimate of coarse root biomass for the study trees using conventional allometric equations from Jenkins et al. (2003) that employed measured DBH and parameters ( $\beta$ ) associated with species class (hardwood or softwood) and species group (hardwoods: *Populus* sp. = “aspen/alder/cottonwood/willow”, *J. nigra* = “mixed hardwood”, and *Q. rubra* = “hard maple/oak/hickory/beech”; softwoods: *P. abies* = “spruce”, and *T. occidentalis* = “cedar/larch”)<sup>2</sup> (Jenkins et al. 2003). The coarse root biomass was estimated such that:

$$\text{BGB}_{\text{ratio}} = \exp(\beta_0 + \beta_1/\text{DBH}) \quad (1)$$

where  $\beta_0$  and  $\beta_1$  are parameters fitted from species class data in Jenkins et al. (2003), DBH is the diameter at breast height (cm), and  $\text{BGB}_{\text{ratio}}$  is the ratio of coarse root biomass to aboveground biomass (AGB), calculated as:

$$\text{AGB} = \exp(\beta_2 + \beta_3 \ln \text{DBH}) \quad (2)$$

where AGB is total aboveground biomass (kg), DBH is the diameter at breast height (cm), and  $\beta_2$  and  $\beta_3$  are parameters fitted from species group data in Jenkins et al. (2003).

#### Root excavations

Following GPR data collection, the belowground root systems of each tree were mechanically excavated using 580 Robert Tire Backhoe. A square plot equivalent to the area scanned with GPR ( $4.5 \times 4.5$  m) was removed of soil and biomass to a depth of 1 m. Coarse roots were manually extracted from the excavated soil. Due to the higher stem density of *T. occidentalis*, roots

were collected for all *T. occidentalis* trees present in the excavated area. One tree replication of *J. nigra* was omitted for concern of inadequate collection of coarse root biomass. For each tree, all coarse roots were weighed for total wet weight. The coarse root gravimetric water content specific to each tree was applied to total wet weight to calculate the total dry weight of the coarse roots ( $\text{kg tree}^{-1}$ ).

#### Root carbon content

Coarse roots were randomly selected during complete excavation. Sample preparation and analysis follow a volatile C-inclusive methodology as suggested by Thomas and Martin (2012) as volatile compounds lost during oven drying constitute a non-negligible amount of C necessary for more accurate C content estimates (Lamlom and Savidge 2003; Thomas and Malczewski 2007; Martin and Thomas 2011). Roots were placed in air-tight bags and transported in a cooler to the laboratory at which point roots were washed to remove soil and stored in air-tight bags at  $-5^\circ\text{C}$ . Coarse roots were cut into cylindrical segments  $\sim 1$  cm in length to retain representative proportions of root tissue. Root samples were dried in an 8 L freeze dryer (Labconco Co., Kansas City, MO, USA) for 7 days. The largest diameter roots were weighed for constant mass on the final day to ensure complete drying.

For each tree species ( $n = 3$ , except *P. abies* and *Populus* sp. where  $n = 2$ ), coarse root samples were prepared as composite samples inclusive of four coarse root diameter classes (0.2–0.5, 0.5–1.0, 1.0–2.0, and  $>2.0$  cm). Samples were ground in a ball grinder (MM400 Mixer Mill; Retsch, Newtown, PA, USA) and stored in snap-cap 1 mL containers at  $-5^\circ\text{C}$ . Total C for each sample was determined using a CHN analyzer (Thermo Flash 2000; Thermo Scientific). Samples were weighed on a microbalance for total sample mass. Elemental analysis calibrations were completed prior to each sample run using aspartic acid. Known standards (SRM 133317, Thermo Scientific) were tested during analysis to confirm instrument accuracy.

As biomass estimates are reported on a dry weight basis, the C concentrations (%) measured from freeze-dried samples were converted onto a dry weight basis:

$$\text{C} = [\text{M}_\text{C} / (\text{M}_\text{F} - (\text{VMF} \times \text{M}_\text{F}))] \times 100 \quad (3)$$

where  $\text{M}_\text{F}$  was the mass of the freeze-dried sample used for elemental analysis and  $\text{M}_\text{C}$  was the mass of C

<sup>2</sup> Due to 1 m stem spacing for *T. occidentalis*, 1 or 2 additional trees were located at the edges of the 3 replicates of the root study area. In order to calculate root biomass in the study area from the allometric equations, these trees were assumed to contribute 50 % of their root biomass into the study area due to their location close to the boundary.

in  $M_F$  (Martin and Thomas 2011). The species' mean volatile mass fraction (VMF) applied to Eq. 3 was the species-specific fraction of biomass lost during heating methods and was calculated as:

$$\text{VMF} = (M_F - M_H) / M_F \quad (4)$$

where an additional subset of freeze-dried samples were weighed ( $M_F$ ) and oven dried at 105 °C for 48 h and weighed again after drying ( $M_H$ ).

Carbon concentration analysis was repeated with oven dried roots to evaluate methodology. Finally, the total root C content for each tree species was calculated by applying the resultant C concentration values of coarse roots to GPR-derived estimates of coarse root biomass.

### Statistical analysis

The GPR index–biomass relationship was developed by regressing the GPR response (area of processed radargrams above an intensity threshold;  $\text{cm}^2$ ) to the coarse root biomass (g) from spatially matched subsurface soil profiles to a depth of 1 m to develop predictive equations. Cook's distance was used to identify potential outliers. One observation representing an excavated soil profile section containing an extremely large *J. nigra* root (>10 cm) of non-cylindrical shape was discarded on this basis. An analysis of covariance (ANCOVA) was used to test for species main effect on biomass as well as the interactive effect of species and GPR signal response (GPR index  $\times$  species) on biomass in order to identify required corrected predictive equations among species.

An assessment of precision of  $B_{\text{GPR}}$  was completed by comparing  $B_{\text{GPR}}$  to the coarse root biomass measured from matched excavated study plots using paired *t* tests on means and a linear regression for all study trees. Differences among species for  $B_{\text{GPR}}$  and C concentration were tested using one-way analysis of variance (ANOVA).

Prior to parametric tests, data were examined for equality of variance using the Bartlett test and for normality of residuals using the Shapiro-Wilks test. Statistical analyses were completed in R v.2.14.2 (R Foundation for Statistical Computing, Vienna, Austria) with the level of significance set at  $P < 0.05$ .

**Table 2** Analysis of covariance for root biomass measured in exposed profiles and GPR response index

	df	SS	MS	F	P
<i>All data</i>					
GPR index	1	25.63	25.63	23.12	<b>&lt;0.0001</b>
Species	4	29.69	7.42	6.70	<b>0.0002</b>
GPR index $\times$ species	4	2.35	0.59	0.53	0.713
Residuals	53	58.74	1.11		
<i>Corrected pooled data without T. occidentalis</i>					
GPR index	1	31.80	31.80	23.735	<b>&lt;0.0001</b>
Species	3	6.52	2.17	1.622	0.198
GPR index $\times$ species	3	2.05	0.68	0.510	0.678
Residuals	43	57.61	1.34		

Displayed are the results for data inclusive of all species and the corrected relationship that removed species main effect on remaining pooled species data. Significant results ( $P < 0.05$ ) are in bold

## Results

### GPR images and index–biomass relationship

Signal noise and planar reflections, specifically from surface reflections, were reduced following the image processing sequence (Fig. 2b, c). Hyperbola migration and the *Hilbert* transformation were successful in emphasizing root reflections in the radargrams (Fig. 2d, e). The selected image intensity threshold (pixel intensity between 175 and 255) delineated these areas of high GPR signal response (Fig. 2f). This allowed for detectable roots to be converted quantitatively to the cross sectional area ( $\text{cm}^2$ ) on the radargram, which became the 'GPR index'. The area bounded in detected root signals within the subset of radargram profiles ranged from 1.56 to 615.44  $\text{cm}^2$ .

Measured coarse root biomass in the exposed soil profiles were positively correlated with the GPR index extracted from the matched radargrams ( $r = 0.47$ ;  $n = 63$ ). However, there was a species main effect on biomass ( $P = 0.0002$ ) (Table 2) that necessitated the development of corrected relationships based on species size. When the data collected for the distinctly smaller *T. occidentalis* were separated from the other four species ('pooled'), the GPR index remained significantly correlated to biomass ( $P < 0.0001$ ). There was no species main effect or GPR index by species interactive effect on biomass for the remaining

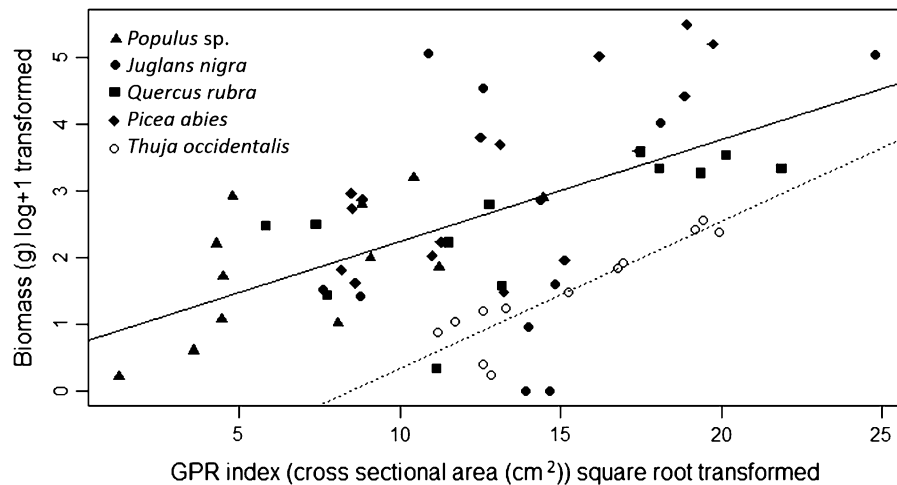


**Fig. 3** Transformed data used to test for species main effect and interactive effect with GPR index on measured biomass (ANCOVA). *Solid symbols* represent corrected pooled species data with no significant species main effect ( $P = 0.20$ ), or

interactive effect with GPR index ( $P = 0.68$ ), on biomass (Table 2). *Open circles* are isolated data points collected below *T. occidentalis* representing the corrected data used for that species GPR index–biomass estimation equation ( $P < 0.0001$ )

pooled species data (Table 2; Fig. 3). The resulting GPR index–biomass predictive equation for the corrected pooled species was  $y = 0.215x - 4.722$  ( $r = 0.55$ ;  $n = 51$ ) and the GPR index–biomass predictive equation of the corrected *T. occidentalis* was  $y = 0.039x - 4.618$  ( $r = 0.95$ ;  $n = 12$ ). These two relational equations were used for biomass estimation at the tree scale.

#### Coarse root biomass

$B_{\text{GPR}}$  was  $54.1 \pm 8.7 \text{ kg tree}^{-1}$  (mean  $\pm$  S.E.) ( $n = 12$ ), regardless of species, and the mean coarse root biomass measured from excavation was  $54.8 \pm 8.3 \text{ kg tree}^{-1}$  ( $n = 12$ ), and not significantly different ( $P = 0.876$ ; Table 3).  $B_{\text{GPR}}$  for *J. nigra* (omitting one excluded individual) closely matched excavated biomass.  $B_{\text{GPR}}$  for *Q. rubra* was a slight overestimate of 4 % and the  $B_{\text{GPR}}$  of *P. abies* was overestimated of 24 %. In contrast, the  $B_{\text{GPR}}$  of *Populus* sp. was  $54.6 \pm 6.0 \text{ kg}$  ( $n = 2$ ) compared to an excavated mean of  $71.9 \pm 10.8 \text{ kg}$  ( $n = 2$ ), an underestimation of 32 %. *Thuja occidentalis* had a  $B_{\text{GPR}}$  of  $11.8 \pm 1.5 \text{ kg tree}^{-1}$  ( $n = 3$ ), an underestimation of the excavated amount by 16 %. The pooled data for  $B_{\text{GPR}}$  and excavated coarse root biomass displayed a linear relationship with no evident bias ( $r^2 = 0.75$ ;  $P = 0.0003$ ) and a root mean square error

(RMSE) of  $14.4 \text{ kg tree}^{-1}$  (Fig. 4). Overall, the estimates derived from the applied allometric equations were less accurate than  $B_{\text{GPR}}$ , underestimating the mean excavated biomass by 19 % (Table 3), and resulting in a weaker correlation ( $r^2 = 0.60$ ; RMSE =  $16.7 \text{ kg tree}^{-1}$ ).

#### Root system carbon content

Among the five species, the concentration of C in the coarse roots was  $45.9 \pm 0.6 \%$  (mean  $\pm$  S.E.;  $n = 5$  species) (Table 4). Carbon concentrations varied from 44.7 to 48.1 % (in *J. nigra* and *P. abies*, respectively), though no significant variation was found among species ( $P = 0.361$ ). Of note, the volatile inclusive methodology captured and additional  $2.1 \pm 0.8 \%$  (mean  $\pm$  S.E.;  $n = 5$  species) of C lost during oven drying methods. The C content of tree root systems using coarse root estimates from GPR data ranged between *T. occidentalis* with  $5.4 \pm 0.7 \text{ kg C tree}^{-1}$  (mean  $\pm$  S.E.;  $n = 3$ ) to *Q. rubra*  $34.8 \pm 6.9 \text{ kg C tree}^{-1}$  ( $n = 3$ ) (Table 4), although no significant variations were detected among species ( $P = 0.361$ ). Overall, the mean C content of tree root systems at this site was estimated at  $25.7 \pm 5.4 \text{ kg C tree}^{-1}$  ( $n = 5$  species), which scales to the landscape level as  $2.9 \text{ Mg C ha}^{-1}$ .



**Table 3** GPR estimated coarse root biomass ( $B_{\text{GPR}}$ ) ( $\text{kg tree}^{-1}$ ; mean  $\pm$  S.E.) with corresponding excavated biomass of five tree species ( $\text{kg tree}^{-1}$ ; mean  $\pm$  S.E)

Tree species	$B_{\text{GPR}}$ ( $\text{kg tree}^{-1}$ )	Excavated ( $\text{kg tree}^{-1}$ )	$n$	$t$ test	$P$ value	Allometric ( $\text{kg tree}^{-1}$ )
<i>Populus</i> sp.	54.6 $\pm$ 6.0	71.9 $\pm$ 10.8	2	-3.60	0.172	90.2 $\pm$ 3.5
<i>Juglans nigra</i>	75.0 $\pm$ 14.4	75.0 $\pm$ 1.4	2	0.003	0.998	56.8 $\pm$ 5.3
<i>Quercus rubra</i>	77.0 $\pm$ 15.4	74.0 $\pm$ 5.7	3	0.296	0.796	44.1 $\pm$ 2.3
<i>Picea abies</i>	62.0 $\pm$ 9.8	50.1 $\pm$ 21.6	2	1.000	0.500	35.9 $\pm$ 12.8
<i>Thuja occidentalis</i> <sup>a</sup>	11.8 $\pm$ 1.5	14.0 $\pm$ 4.0	3	-0.403	0.726	12.3 $\pm$ 4.7
All study trees	54.1 $\pm$ 8.7	54.8 $\pm$ 8.3	12	-0.160	0.876	44.6 $\pm$ 7.9

Paired  $t$  tests completed on the means between  $B_{\text{GPR}}$  and excavated biomass for each species and across all study trees. Also shown are corresponding calculated allometric estimates of coarse root biomass as a function of DBH and the species' class and group [allometric estimates based on equations from Jenkins et al. (2003)]

<sup>a</sup> *T. occidentalis* is based on an area not an individual tree basis, where root area is equivalent to the other tested tree species individual root biomass area ( $4.5 \times 4.5$  m)

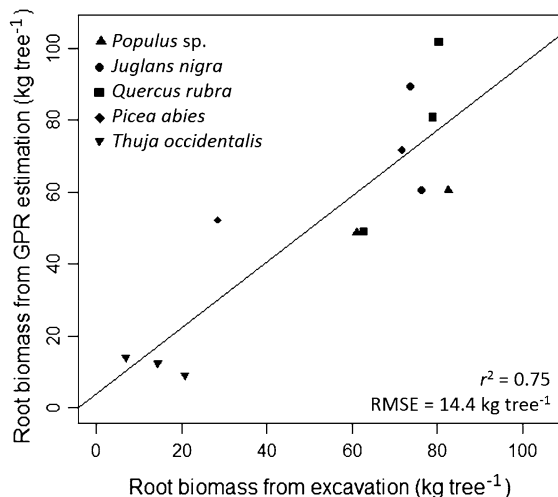


**Fig. 4** Positive correlation (solid line) between coarse root biomass estimated by GPR ( $\text{kg tree}^{-1}$ ) and coarse root biomass measured from matched excavations ( $\text{kg tree}^{-1}$ ) ( $r^2 = 0.75$ ;  $P = 0.0003$ ;  $\text{RMSE} = 14.4 \text{ kg tree}^{-1}$ ;  $n = 12$ ).  $B_{\text{GPR}}$  for *T. occidentalis* is based on an area not an individual tree basis, where root area is equivalent to the other tested tree species individual root biomass area ( $4.5 \times 4.5$  m)

## Discussion

### The GPR–biomass relationship

The use of a linear GPR index–biomass relationship was suitable in this study due to low variability of coarse root water content (Guo et al. 2013c) and a large difference between root and soil water contents (Hirano et al. 2009). A correlation of  $r = 0.89$  between biomass from soil cores and GPR index was

found in a study completed by Samueslon et al. (2008). They used a 1.5 GHz GPR unit in a *Pinus taeda* plantation on sandy loam soils and correlated subsurface data exclusively to a depth of 30 cm. The correlation from Day et al. (2013), also using a 1.5 GHz GPR unit, was  $r = 0.69$  between biomass from soil cores and a GPR index inclusive of subsurface data to a depth of 60 cm in a scrub-oak ecosystem co-dominated by *Quercus myrtifolia* and *Quercus geminata* on sandy soils in Florida, USA. Although it should be expected that GPR index–biomass correlations will be reduced when there is an increase of depth of radar analysis and an increase of the variability in subsurface conditions, here we include roots to a depth of 1 m while still maintaining a reasonably strong correlation ( $r = 0.55$ ) inclusive of four different tree species. The corrected relationship for *T. occidentalis* showed a very strong correlation ( $r = 0.95$ ) in part due to the shallower root system of this relatively smaller tree species.

Ideally, the utility of GPR biomass estimation across a landscape would be greater given the applicability of one GPR index–biomass relationship to apply to all radargram data. This would reduce the number of biomass calibration points and, in scenarios where trees are proximal, overcome the limitations of determining species-specific roots detected by GPR. However, from the results of this study, two predictive equations that differentiate between the larger deep-rooted species and the smaller shallow-rooted species were appropriate in order to remove species effects. Similarly, Butnor et al. (2003) developed corrected relationships of GPR index–biomass for two

**Table 4** Carbon concentration (%) and C content (kg C tree<sup>-1</sup>) of the coarse root system of five tree species (25-years-old)

Tree species	C concentration of coarse roots (%) (1) conventional dry	C concentration of coarse roots (%) (2) volatile inclusive	Coarse root C content from B <sub>GPR</sub> (kg C tree <sup>-1</sup> )	Coarse root C content at site level (Mg C ha <sup>-1</sup> )
<i>Populus</i> sp.	43.6 ± 2.1	45.8 ± 1.1	25.0 ± 2.7	2.8
<i>Juglans nigra</i>	44.5 ± 1.0	44.7 ± 0.3	33.5 ± 6.4	3.7
<i>Quercus rubra</i>	42.2 ± 0.2	45.2 ± 1.0	34.8 ± 6.9	3.9
<i>Picea abies</i>	47.8 ± 1.2	48.1 ± 0.6	29.8 ± 4.7	3.3
<i>Thuja occidentalis</i>	41.4 ± 0.4	45.8 ± 2.3	5.4 ± 0.7 <sup>a</sup>	0.6
Average ( <i>n</i> = 5 species)	42.2 ± 1.1	45.9 ± 0.6	25.7 ± 5.4	2.9

Carbon concentration values are reported as total carbon of dry root weight (mean ± S.E.) (*n* = 3, except *Populus* sp. and *P. abies* *n* = 2) following (1) conventional oven dry sample preparation or (2) volatile inclusive methodology. Carbon content of the trees' root systems were calculated using B<sub>GPR</sub> and the species-specific coarse root C concentration (volatile inclusive) and reported on a tree basis as well as a site level using a previously reported stem density of 111 trees ha<sup>-1</sup> (Peichl et al. 2006)

<sup>a</sup> Reporting kg of C on an area basis (kg C root area<sup>-1</sup>), where root area is equivalent to the other tested tree species individual root biomass area (4.5 × 4.5 m)

contrasting scenarios of fertilizer use or no fertilizer use in a *Pinus taeda* stand, which altered the soil conditions for radar signals. Given reasonably consistent subsurface conditions (e.g. clay content) and soil-root moisture gradients, corrected GPR index–biomass relationships may be required for scenarios of distinct biomass gradients, a reality for temperate TBI systems.

#### Biomass and carbon estimates of tree root systems

Inclusion of the fraction of volatile C lost during high-heat (105 °C) drying improved accuracy of C content estimates. The highest root C concentration was for coniferous *P. abies*, consistent with previous reported trends where coniferous trees have a higher concentration of C than deciduous trees in temperate regions (IPCC 2006; Thomas and Martin 2012). Peichl et al. (2006) reported coarse root C concentrations, using conventional oven-drying methods, of 13-year-old *P. abies* at 51 %, which is ~3 % greater than those found in our study. Conversely, carbon concentrations for *Populus* sp. roots found by Peichl et al. (2006) (43 %) were ~3 % lower than our reported values inclusive of volatiles, but similar to the results from oven dry methods. Bert and Danjon (2006) detected variation between the interior root “wood” and the exterior root “bark” (bark + phloem) of *Pinus pinaster* Ait., with the root bark ~3 % greater in concentration. They also reported diameter-dependent

variation notably for roots <4 cm (Bert and Danjon 2006). We did not test for variation within root tissues, but acknowledge that there may be within-root variation of C concentrations dependent on the ratio of root components, which would be inherently affected by the diameter of root samples used during elemental analysis. Additional sources of variability in C concentration of tree roots may arise from variation in sampling and C analysis protocol as well as physiological variation (Lamlom and Savidge 2003), such as tree root carbohydrate storage (Bert and Danjon 2006).

In order to show the C storage potential of trees in temperate tree-based intercropping systems, system level root C quantification was calculated using the current hardwood tree density of 111 trees ha<sup>-1</sup>. However, it should be noted that if only coniferous trees are integrated, the tree density will be much higher due to lower spacing used for coniferous trees. The estimated root C content at this site indicates an increase of belowground C storage over the last 12 years when compared to the root C content of the average reported values for 13-year-old *Populus* sp. and *P. abies* at the same site (1.8 Mg C ha<sup>-1</sup>) (Peichl et al. 2006). In temperate TBI systems, stem density, species composition, and the age of trees are highly variable. Thus reporting species root biomass and root C content at the tree scale is valuable for operational purposes that are specific to these variables (Thevathasan and Gordon 2004).

## Application and limitations of GPR in tree-based intercropping

There are limitations to biomass components GPR can detect. Coarse roots smaller than 1.0 cm in diameter are less likely to cause radar signal response than larger roots ( $\geq 1$  cm) (Hirano et al. 2012), coarse roots located deeper than GPR signal penetration can be undetected or misinterpreted by the GPR signal response (Hirano et al. 2009), and coarse roots located outside of the field of the radar signals, such as directly below the stem, will be undetected (Samuelson et al. 2008). As a result of these detection limitations there is an anticipated bias towards GPR underestimation of coarse root biomass, assuming proper calibration and appropriate conditions. With the exception of *Populus* sp., this bias was not observed in our results suggesting that the subsurface conditions and the morphological characteristics (e.g. tap roots growing horizontal from the stem) of the root systems at this study site were conducive for radar study. However, some detected biomass might be attributed to false positive GPR signal response incurred from in-field conditions.

Although GPR does require some destructive calibration sampling using soil cores or partial excavations, the amount of physical sampling required to estimate the coarse root biomass is drastically reduced compared to conventional studies in TBI systems. During the current study, 243 m<sup>2</sup> of surface area were scanned with GPR, an area equating to over 13,500 soil cores (of 15 cm diameter). GPR techniques can provide more thorough understanding of the heterogeneity of the root systems without total excavation in agroforestry systems (Isaac et al. 2014) and unlike destructive sampling, this method of root data collection can be repeated, critical for temporal-scale studies on root system dynamics (Norby and Jackson 2000). We tested the use of pre-established species-based allometric and root:shoot equations, a more traditional approach to quantify root biomass, and found that these produced less accurate estimates of the excavated root biomass compared to the GPR estimates. Generalized equations derived from forest ecosystem data might be unsuitable for trees in agricultural landscapes where variation in management (e.g. planting density and fertilizer application) can induce differences in biomass allocation. Results from this study suggest that the overall accuracy of the allometric estimates was outperformed by GPR estimations

and support the need for more site- and species-specific tree root data. Recent advancements in modelling radar signal response given variable root and soil conditions have been reported following controlled experiments (Guo et al. 2013b; Tanikawa et al. 2013). With these advancements, there is potential of enhancing accuracy of root estimation for in-field conditions and lessening the need for destructive sampling for calibrations.

## Conclusions

Coarse root biomass of 12 trees, inclusive of five species, was accurately estimated with the use of GPR at a TBI site in Southern Ontario, Canada. Subsequently, C content of tree root systems was quantified using species-specific coarse root C concentrations. This was the first in-field study to test the robustness of GPR as a coarse root biomass estimation tool across multiple species. Corrected predictive relationships between GPR signal response and root biomass were required to remove a strong species effect, namely isolating data from a species with a distinctly smaller and shallower root system. We argue that this technology can be suitable for use in temperate TBI systems under well-drained, sandy loam soils. Ultimately, these results contribute to furthering methodological techniques of GPR root study for direct quantification of belowground biomass and C storage in agroforestry systems and other tree-based ecosystems.

**Acknowledgments** We would thank the faculty, staff, and students at the University of Guelph Agroforestry Research Station. Amy Wotherspoon from the University of Guelph graciously provided root excavation data and Stephanie Gagliardi provided important assistance during field work and laboratory analysis. We also thank Tom Meulendyk for assistance. We thank two anonymous journal reviewers for their insightful and constructive comments on earlier versions of the manuscript. Funding was provided by the Faculty of Forestry at the University of Toronto, Agriculture and Agri-Food Canada's Agricultural Greenhouse Gases Program, and the Natural Sciences and Engineering Research Council of Canada.

## References

- Bambrick AD, Whalen JK, Bradley RL, Cogliastro A, Gordon AM, Olivier A, Thevathasan NV (2010) Spatial heterogeneity of soil organic carbon in tree-based intercropping

- systems in Quebec and Ontario, Canada. *Agrofor Syst* 79:343–353
- Barton CVM, Montagu KD (2004) Detection of tree roots and determination of root diameters by ground penetrating radar under optimal conditions. *Tree Physiol* 24:1323–1331
- Bert D, Danjon F (2006) Carbon concentration variations in the roots, stem and crown of mature *Pinus pinaster* (Ait.). *For Ecol Manag* 222:279–295
- Brunner I, Godbold DL (2007) Tree roots in a changing world. *J For Res* 12:78–82
- Butnor JR, Doolittle JA, Kress L, Cohen S, Johnsen KH (2001) Use of ground-penetrating radar to study tree roots in the southeastern United States. *Tree Physiol* 21:1269–1278
- Butnor JR, Doolittle JA, Johnsen KH, Samuelson L, Stokes T, Kress L (2003) Utility of ground-penetrating radar as a root biomass survey tool in forest systems. *Soil Sci Soc Am J* 67:1607–1615
- Cairns MA, Brown S, Helmer EH, Baumgardner GA (1997) Root biomass allocation in the world's upland forests. *Oecologia* 111:1–11
- Cui X, Guo L, Chen J, Chen X, Zhu X (2013) Estimating tree-root biomass in different depths using ground-penetrating radar: evidence from a controlled experiment. *IEEE Trans Geosci Remote Sens* 51:3410–3423
- Dannoura M, Hirano Y, Igarashi T, Ishii M, Aono K, Yamase K, Kanazawa Y (2008) Detection of *Cryptomeria japonica* roots with ground penetrating radar. *Plant Biosyst* 142:375–380
- Davis JL, Annan AP (1989) Ground-penetrating radar for high-resolution mapping of soil and rock stratigraphy. *Geophys Prospect* 37:531–551
- Day FP, Schroeder RE, Stover DB, Brown ALP, Butnor JR, Dilustro J, Hungate BA, Dijkstra P, Duval BD, Seiler TJ, Drake BG, Hinkle CR (2013) The effects of 11 yr of CO<sub>2</sub> enrichment on roots in a Florida scrub-oak ecosystem. *New Phytol* 200:778–787
- Dixon RK, Winjum JK, Andrasko KJ, Lee JJ, Schroeder PE (1994) Integrated land-use systems: assessment of promising agroforest and alternative land-use practices to enhance carbon conservation and sequestration. *Clim Change* 27:71–92
- Guo L, Chen J, Cui X, Fan B, Lin H (2013a) Application of ground penetrating radar for coarse root detection and quantification: a review. *Plant Soil* 362:1–23
- Guo L, Lin H, Fan B, Cui X, Chen J (2013b) Forward simulation of root's ground penetrating radar signal: simulator development and validation. *Plant Soil*. doi:10.1007/s11104-013-1751-8
- Guo L, Lin H, Fan B, Cui X, Chen J (2013c) Impact of root water content on root biomass estimation using ground penetrating radar: evidence from forward simulations and field controlled experiments. *Plant Soil*. doi:10.1007/s11104-013-1710-4
- Hirano Y, Dannoura M, Aono K, Igarashi T, Ishii M, Yamase K, Makita N, Kanazawa Y (2009) Limiting factors in the detection of tree roots using ground-penetrating radar. *Plant Soil* 319:15–24
- Hirano Y, Yamamoto R, Dannoura M, Aono K, Igarashi T, Ishii M, Yamase K, Makita N, Kanazawa Y (2012) Detection frequency of *Pinus thunbergii* roots by ground-penetrating radar is related to root biomass. *Plant Soil* 360:363–373
- Hruska J, Čermák J, Sustek S (1999) Mapping tree root systems with ground-penetrating radar. *Tree Physiol* 19:125–130
- IPCC (2006) Intergovernmental panel on climate change guidelines for national greenhouse gas inventories. Chapter 4: Forest lands. National greenhouse gas inventories programme, Japan
- Isaac ME, Anglaaere LCN (2013) An in situ approach to detect tree root ecology: linking ground-penetrating radar imaging to isotope-derived water acquisition zones. *Ecol Evol* 3:1330–1339
- Isaac ME, Gordon AM, Thevathasan N, Oppong SK, Quashie-Sam J (2005) Temporal changes in soil carbon and nitrogen in west African multistrata agroforestry systems: a chronosequence of pools and fluxes. *Agrofor Syst* 65:23–31
- Isaac ME, Anglaaere LCN, Borden KA, Adu-Bredu S (2014) Intraspecific root plasticity in agroforestry across edaphic conditions. *Agric Ecosyst Environ* 185:16–23
- Jackson RB, Canadell J, Ehleringer JR, Mooney HA, Sala OE, Schulze ED (1996) A global analysis of root distributions for terrestrial biomes. *Oecologia* 108:389–411
- Jenkins JC, Chojnacky DC, Heath LS, Birdsey RA (2003) National-scale biomass estimators for united states tree species. *For Sci* 49:12–35
- Jose S (2009) Agroforestry for ecosystem services and environmental benefits: an overview. *Agrofor Syst* 76:1–10
- Jose S, Gillespie AR, Pallardy SG (2004) Interspecific interactions in temperate agroforestry. *Agrofor Syst* 61:237–255
- Kessler M, Hertel D, Jungkunst HF, Kluge J, Abrahamczyk S, Bos M, Buchori D, Gerold G, Gradstein SR, Köhler S, Leuschner C, Moser G, Pitopang R, Saleh S, Schulze SH, Sporn SG, Steffan-Dewenter I, Tjitrosoedirdjo SS, Tschamtko T (2012) Can joint carbon and biodiversity management in tropical agroforestry landscapes be optimized? *PLoS ONE* 7:e47192
- Kirby KR, Potvin C (2007) Variation in carbon storage among tree species: implications for the management of a small-scale carbon sink project. *For Ecol Manag* 246:208–221
- Kurz WA, Beukema SJ, Apps MJ (1996) Estimation of root biomass and dynamics for the carbon budget model for the Canadian forest sector. *Can J For Res* 26:1973–1979
- Kuyah S, Dietz J, Muthuri C, Jamnadass R, Mwangi P, Coe R, Neufeldt H (2012) Allometric equations for estimating biomass in agricultural landscapes: II. Belowground biomass. *Agric Ecosyst Environ* 158:225–234
- Lamlom SH, Savidge RA (2003) A reassessment of carbon content in wood: variation within and between 41 North American species. *Biomass Bioenergy* 25:381–388
- Martin AR, Thomas SC (2011) A reassessment of carbon content in tropical trees. *PLoS ONE* 6:e23533
- Mokany K, Raison RJ, Prokushkin AS (2006) Critical analysis of root:shoot ratios in terrestrial biomes. *Glob Change Biol* 12:84–96
- Moser G, Leuschner C, Hertel D, Hölscher D, Köhler M, Leitner D, Michalzik B, Prihastanti E, Tjitrosemto S, Schwendenmann L (2010) Response of cocoa trees (*Theobroma cacao*) to a 13-month desiccation period in Sulawesi, Indonesia. *Agrofor Syst* 79:171–187
- Nair PKR, Kumar BM, Nair VD (2009) Agroforestry as a strategy for carbon sequestration. *J Plant Nutr Soil Sci* 172:10–23

- Nair PKR (2011) Carbon sequestration studies in agroforestry systems: a reality-check. *Agrofor Syst* 86:243–253
- Norby RJ, Jackson RB (2000) Root dynamics and global change: seeking an ecosystem perspective. *New Phytol* 147:3–12
- Oelbermann M, Voroney RP (2007) Carbon and nitrogen in a temperate agroforestry system: using stable isotopes as a tool to understand soil dynamics. *Ecol Eng* 29:342–349
- Oelbermann M, Voroney RP, Gordon AM (2004) Carbon sequestration in tropical and temperate agroforestry systems: a review with examples from Costa Rica and southern Canada. *Agric Ecosyst Environ* 104:359–377
- Oelbermann M, Voroney RP, Kass DCL, Schlönvoigt AM (2005) Above- and below-ground carbon inputs in 19-, 10- and 4-year-old Costa Rican Alley cropping systems. *Agric Ecosyst Environ* 105:163–172
- Peichl M, Thevathasan NV, Gordon AM, Huss J, Abohassan RA (2006) Carbon sequestration potentials in temperate tree-based intercropping systems, Southern Ontario, Canada. *Agrofor Syst* 66:243–257
- Polomski J, Kuhn N (2002) Root research methods. In: Waisel Y, Eshel A, Kafkafi U (eds) *Plant roots the hidden half*, 3rd edn. Marcel Dekker, New York, pp 295–321
- Price GW, Gordon AM (1999) Spatial and temporal distribution of earthworms in a temperate intercropping system in southern Ontario, Canada. *Agrofor Syst* 44:141–149
- Raz-Yaseef N, Koteen L, Baldocchi DD (2013) Coarse root distribution of a semi-arid oak savanna estimated with ground penetrating radar. *J Geophys Res Biogeosci* 118:135–147
- Samuelson LJ, Butnor J, Maier C, Stokes TA, Johnsen K, Kane M (2008) Growth and physiology of loblolly pine in response to long-term resource management: defining growth potential in the southern United States. *Can J For Res* 38:721–732
- Samuelson LJ, Eberhardt TL, Butnor JR, Stokes TA, Johnsen KH (2010) Maximum growth potential in loblolly pine: results from a 47-year-old spacing study in Hawaii. *Can J For Res* 40:1914–1929
- Schroth G (1999) A review of belowground interactions in agroforestry, focussing on mechanisms and management options. *Agrofor Syst* 43:5–34
- Schroth G, Kolbe D (1994) A method of processing soil core samples for root studies by subsampling. *Biol Fertil Soils* 18:60–62
- Stover DB, Day FP, Butnor JR, Drake BG (2007) Effect of elevated CO<sub>2</sub> on coarse-root biomass in Florida scrub detected by ground-penetrating radar. *Ecol* 88:1328–1334
- Tanikawa T, Hirano Y, Dannoura M, Yamase K, Aono K, Ishii M, Igarashi T, Ikeno H, Kanazawa Y (2013) Root orientation can affect detection accuracy of ground-penetrating radar. *Plant Soil*. doi:10.1007/s11104-013-1798-6
- Taylor BN, Beidler KV, Cooper ER, Strand AE, Pritchard SG (2013) Sampling volume in root studies: the pitfalls of under-sampling exposed using accumulation curves. *Ecol Lett* 16:862–869
- Thevathasan NV, Gordon AM (2004) Ecology of tree intercropping systems in the North temperate region: experiences from southern Ontario, Canada. *Agrofor Syst* 61:257–268
- Thomas SC, Malczewski G (2007) Wood carbon content of tree species in Eastern China: interspecific variability and the importance of the volatile fraction. *J Environ Manag* 85:659–662
- Thomas SC, Martin AR (2012) Carbon content of tree tissues: a synthesis. *For* 3:332–352
- Vogt KA, Vogt DJ, Bloomfield J (1998) Analysis of some direct and indirect methods for estimating root biomass and production of forests at an ecosystem level. *Plant Soil* 200:71–89